PPgMA/APTS Compound Coupling Compatabilizer in PP/Clay Hybrid Nanocomposite

Wen-Chang Liaw,[1] Po-Chen Huang,[1] Chee-Shan Chen,[2] Chi-Lang Lo,[1] Ju-Liang Chang[1]

[1]*Department of Chemical Engineering, National Yunlin University of Science and Technology, Yunlin 640, Taiwan, Republic of China*
[2]*Department of Applied Chemistry, Chaoyang University of Technology, Taichung County 413, Taiwan, Republic of China*

Received 8 June 2007; accepted 31 January 2008
DOI 10.1002/app.28294
Published online 29 April 2008 in Wiley InterScience (www.interscience.wiley.com).

ABSTRACT: A compound coupling compatibilizer employing coupled use of γ-(aminopropyl) triethoxy silane (APTS) and maleic anhydride-*graft*-polypropylene (PPgMA) was synthesized for the preparation of polypropylene (PP)/clay hybrid nanocomposites. The designed PPgMA/APTS compound coupling compatabilizer, through condensation of the amino groups of APTS with the anhydride groups of MA moieties in PPgMA, is capable of forming chemical bonding with the organo clay (org-clay) while maintaining compatibility with the organic PP compartment. Various PPgMA to APTS ratios of these compound coupling compatibilizers were first reacted with clay to form PPgMA/clay masterbatches. The obtained masterbatches were then compounded with PP to produce PP/clay hybrid nanocomposites possessing different characteristics. The composition effects were studied. For org-clay content of 5 wt %, intercalated-exfoliated structure of the nanocomposite could be maintained for better reinforcement. T_d of 484°C was achieved, indicating significant improvement over neat PP (T_d was 386°C) in thermal property. The ultimate tensile strength (30% higher than control) and Young's modulus (57% higher than control) measurements also justified the application of the PPgMA/APTS compound coupling compatibilizer in the incorporation of org-clay in PP matrix. The use of the PPgMA/APTS compound coupling compatibilizer can provide design flexibility in manufacturing PP/clay hybrid nanocomposites. © 2008 Wiley Periodicals, Inc. J Appl Polym Sci 109: 1871–1880, 2008

Key words: poly(propylene)PP; silane coupling agent; nanocomposites; clay; inorganic materials

INTRODUCTION

The organic–inorganic nanocomposites have attracted great interest, both in industry and in academia, because they often exhibit a wide range of enhanced mechanical, thermal, and other properties when compared with plain polymers or conventional micro and macrocomposites.[1–4]

One of the most promising nanocomposite systems would be a hybrid based on organic polymers and inorganic clay minerals consisting of layered silicate.[5–9] Ever since a polymer/clay nanocomposite system of polyamide 6/clay was synthesized by a group at the Toyota Research Center in Japan,[10–12] several polymer nanocomposites have been reported up to date; they are nanocomposites of poly(ethylene terephthalate),[13–15] poly(methyl methacrylate),[16–19] polyurethane,[20] and epoxy resins.[21]

As stated by López-Quintanilla et al. in their report,[22] three types of polymer/clay composites are usually recognized: ''conventional composites,'' in which the clay was added as common filler; ''intercalated nanocomposites,'' in which a small portion of polymer was allowed to insert into the interlayer spacing between the layered silicates, and ''exfoliated nanocomposites,'' in which the layered silicates are well dispersed in a continuous polymer matrix.[23,24]

Polypropylene (PP) is one of the most widely used polyolefin polymers due to its low cost, low density, high heat distortion temperature (above 100°C), and extraordinary versatility in terms of application and recycling. However, there is still room for improvements in terms of toughness and thermal stability of PP. Nanotechnology has been applied, in this field, in an effort to further improve properties of PP.

In such nanotechnology, clay mineral is one of the most commonly used nanofiller. However, before incorporating into the hydrophobic PP polymer matrix, the clay needs to be modified for hydrophobicity of the clay's surface, also, for expanding the spaces between the silicate layers. This kind of modified clay is commonly called organo-clay (org-clay).

On the other hand, PP does not have polar groups in its backbone, and nonpolar nature makes it incompatible with clay. To achieve nanomeric

Correspondence to: W.-C. Liaw (liawwc@yuntech.edu.tw).

dispersion of the org-clay, the modification of PP matrix with polar molecules is recommended prior to org-clay incorporation.[22,25] On the way to finding methods for nanomeric dispersion, the use of polar functional polymeric compatibilizer in the preparation of materials such as PP/clay nanocomposites, has been suggested.[26–29] In such design, the polar functional groups of the functional polymer was expected to have strong interaction with the org-clay, while the polymer segment itself is miscible or compatible with the bulk polymer matrix.

Usuki et al.[30] first reported an approach to prepare PP nanocomposites using a functional compatibilizer (PP—OH) with polar telechelic OH groups to increase compatibility. García-López et al.[31] compared two functional polymers: diethyl maleated grafted PP (PPgDEM) and maleic anhydride-grafted PP (PPgMA), for their use as compatibilizer. They concluded that diethyl maleate, which was less polar than maleic anhydride, and PPgMA provided a more effective interaction with the polar hydroxyl group of the org-clay.

López-Quintanilla et al.[22] reported that gracidyl methacrylate grafted PP (PPgGMA) and PPgMA were better compatibilizing agent than acrylic acid grafted PP (PPgAA). They concluded that the former two groups, as a result of better interfacial adhesion, were shown to have better mechanical performance.

It is a general concord that if the nanocomposites were formed by covalent bonding between organic polymers and the relatively inorganic clay, the interfacial attraction between these two phases would become stronger and the thermal and mechanical properties of the nanocomposites would be enhanced.

Liu and Wu[18] used epoxy propyl methacrylate to prepare a cointercalation organophilic clay which displayed a larger interlayer spacing and stronger interaction with the PP than did ordinary alkylammonium-modified ''organophilic'' clay. Unsaturated cointercalation monomer was used so that it could attach to the PP backbone by virtue of a grafting reaction.

Wu et al.[32] prepared hexamethylene diamine (HMDA)-modified PPgMA/clay nanocomposites, in that the HMDA was grafted with the PPgMA and the resulting polymer (designated as PPgHMA) was then mixed with the organically modified montmorillonite (MMT) in hot xylene solution. These PPgHMA/clay nanocomposites contained fully exfoliated and randomly distributed silicate layers within a PPgHMA matrix.

There were other reports which discussed the incorporation of silane coupling agents in the preparation of polymer/clay nanocomposites for increasing the organic inorganic interaction. These included γ-methacryloxy propyl trimethoxysilane,[33–37] isobutyl trimethoxysilane,[38] and trimethylchlorosilane.[39]

Rong et al.[33] developed an effective surface modification method on the alumina nanoparticles to enhance the interfacial interaction in alumina nanoparticles filled polymer composites. In their work, the alumina surface was first treated with γ-methacryloxypropyl trimethoxysilane, followed by radical grafting polymerization with polystyrene and polyacrylamide in either aqueous or nonaqueous system. Results of infrared spectroscopy and dispersiveness studies in solvent showed that the desired polymer chains were covalently bonded to the surface of the alumina particles.

Seckin et al.[37] reported the preparation of a natural clay–polymer hybrid material from natural bentonite that was modified with silane-coupling agent, γ-methacryloxypropyl trimethoxysilane, followed by copolymerization with acrylonitrile. According to their report, the particle surface was either physically bound by entanglement or chemically bound by covalent bonding to the silane.

Wang and Sheng[34,35] have prepared another type of ''organophilic'' clay, attapulgite, first by γ-methacryloxypropyl trimethoxysilane modification, and then graft-polymerization with butyl acrylate. The dried organophilic attapulgite-polybutyl acrylate hybrid material was then melt-blended with PP to obtain PP-attapulgite nanocomposites. The strength and stiffness of these nanocomposites were both improved significantly in the presence of organic attapulgite.

In the above cited references, the silane coupling agents could be characterized by the presence of an active trialkoxysilyl group which chemically interacts with the virtually inorganic clay to form the Si—O—Si covalent bonding. These coupling agents can further be classified into two types, according to their functionalities at the other end (the organic terminal) of the coupling agent: one was attached with a reactive methacryloyl group, and the other was ended with an inactive organic group (e.g., isobutyl,[38] trimethylsilyl[39]). Utilizing the reactive methacryloyl group (methacryloxy propyl trimethoxysilane), the first type of coupling agent can be activated by radicals to initiate grafting with polystyrene and polyacrylamide,[33] or alternatively, copolymerized with acrylonitrile[37] or butyl acrylate.[34,35] The second type assisted in compatibilizing the organic polymer through dispersion forces.

In this study, we proposed the use of the well-available and inexpensive silane coupling agent of 3-(aminopropyl) triethoxy silane (APTS) and its incorporation in PP-clay nanocomposite. The choice of this coupling agent is based on its amino group that can form an amide linkage, through condensation, with the maleic anhydride moiety of PPgMA.[40] Such compounded use of APTS and PPgMA has two advantages: one is that its triethoxy silyl group is capable of reacting with the hydroxyl group on the edges of clay

to form a covalent linkage between PPgMA and clay, and the other being that the PP segment of PPgMA can be thoroughly compatibilized with PP matrix by entanglement. Hopefully, this may render the nanocomposite material increased interaction and dispersion of the clay in the polymer matrix, and therefore, more design flexibilities.

The preparation process that we proposed involves three steps.[22,41,42] First, APTS was allowed to react with PPgMA to form the compound coupling compatibilizer. Second, the PPgMA/APTS compound coupling compatibilizer was allowed to react with the org-clay to form a hybrid masterbatch. Third, the masterbatch was then compounded with pure PP to form the nanocomposite.

The chemical structure, morphology, thermal and dynamic mechanical properties of the prepared PP/clay nanocomposites will be investigated by a series of physical and chemical measurements.

TABLE I
Compositions of the PPgMA/Clay Masterbatch and PP/Clay Nanocomposites

Ingredient of masterbatch				
Clay (wt %)	PPgMA (wt %)	APTS (wt %)	PP (wt %)	PP/clay code
1	5	1	93	PMC-a1
3	5	1	91	PMC-a3
5	5	1	89	PMC-a5
7	5	1	87	PMC-a7
1	10	1	88	PMC-b1
3	10	1	86	PMC-b3
5	10	1	84	PMC-b5
7	10	1	82	PMC-b7
1	20	1	78	PMC-c1
3	20	1	76	PMC-c3
5	20	1	74	PMC-c5
7	20	1	72	PMC-c7
1	10	0	89	PMC-b01
3	10	0	87	PMC-b03
5	10	0	85	PMC-b05
7	10	0	83	PMC-b07

EXPERIMENTAL

Materials

Purified sodium MMT, with a cation exchange capacity of 105 mequiv/100 g was obtained from Paikong Nanotechnology (Tao Yuan, Taiwan). Octadecyl trimethyl ammonium chloride (OTAC) was purchased from Taiwan Surfactant Corp. (Taipei, Taiwan). PP (no. 366-3) was purchased from Taiwan Polypropylene (Taipei, Taiwan), and its melt index was 3.0 g/10 min [according to American Society for Testing and Materials (ASTM) D 1238]. PPgMA (MA content: 0.6 wt %) was purchased from Aldrich (Milwaukee, WI), and its melt index (190°C/2.16 kg) was 115 g/10 min. The APTS was obtained from Shin-Etsu Silicone Taiwan (Taipei, Taiwan).

Preparation of organophilic clay

Purified sodium-MMT (10 g) was dispersed into 2000 mL of hot water (80°C) in a high speed mixer. OTAC (45 g) was dissolved in hot water, then poured into the MMT-water suspension solution under vigorous stirring for 30 min, and a white precipitate was obtained. The precipitate was collected by filtration and washed with hot ethanol/H_2O (1 : 1 weight) several times to make sure that the product was free of chloride ion. The product was dried at 100°C in vacuum for 6 h and was designated as org-clay. The interlayer spacing of the OTAC-modified org-clay was about 20.4 Å, measured by X-ray diffraction (XRD).

Preparation of covalently bonded PPgMA/clay masterbatch

A xylene solution of PPgMA was prepared by dissolving various amount of PPgMA in 50 mL of xylene under reflux (Table I). After complete dissolution of PPgMA in xylene (1.5 h), APTS was added into the hot xylene solution of PPgMA at 80°C with stirring. Another org-clay suspension solution was prepared by dispersing various amount of org-clay (Table I) into xylene and heated to 80°C with stirring for 1 h until the org-clay suspension solution became clear. The xylene suspension solution of org-clay was added into the above solution of the condensation reaction product of PPgMA and APTS at 80°C.

Methanol and water, in an amount about 4× that of APTS (w/w) in acidic condition, was added to the above mixture for another condensation reaction. The mixture was allowed to react for 3 h, for Si—O—Si bond formation between the triethylsilyl group of APTS and the Si—OH group of the org-clay. The products were precipitated in an excess amount of methanol and the precipitate was filtered. The collected products were redissolved in xylene, precipitated in excess methanol, and filtered again, and this process was repeated three times. The obtained covalently bonded PPgMA/clay masterbatch was dried at 80°C under vacuum. The compositions of PPgMA/clay masterbatch at various designed ratios of ingredients are summarized in Table I.

Preparation of PP/clay nanocomposites

Various amount of PP was dissolved in xylene under reflux and stirred for 1.5 h, for complete dissolution. The PPgMA/clay masterbatch was then added into this refluxing PP solution and stirred for another 1.5 h. The resulting PP/clay nanocomposite solution was precipitated in an excess amount of methanol, filtered, and washed with xylene and methanol for

three times. Finally, the obtained PP/clay nanocomposites were dried at 80°C under vacuum. The compositions of PP/clay nanocomposites at various designed ratios of ingredients are shown in Table I.

Characterization

Fourier transform infrared (FTIR) absorption spectra were recorded between 600 and 4000 cm^{-1} by using a Bruker ISF 112 V FTIR spectrometer. XRD analysis was carried out with a Rigaku model D/MAX 2500 instrument equipped with a Cu Kα radiation source. The transmission electron microscopy (TEM) observation was performed on an ultrathin film with a JEOL EM9110MEGA instrument using an acceleration voltage of 120 kV. The thermal stability of the nanocomposites was characterized with a thermogravimetric analyzer (TGA), on a TA Instruments Q500 system under a nitrogen environment. The heating process was conducted from 25 to 900°C at a rate of 20°C/min. The studies of melting and crystallization behaviors of the nanocomposites were carried out with a Perkin–Elmer DSC-7 differential scanning calorimeter (DSC). About 8 mg of the specimens were sealed into an aluminum pan in DSC studies. The temperature was raised from 30 to 200°C at a rate of 20°C/min under nitrogen atmosphere. The specimens were held at 200°C for 10 min to minimize the effect of heating history before cooling at a rate of 20°C/min.

The dynamic mechanical properties of the tensile-molded samples were measured with a TA DMA-2900 system. The vibration frequency was 1 Hz in a nitrogen atmosphere and the temperatures ranged from 0 to 140°C at a heating rate of 3°C/min. The studies of mechanical properties were carried out using a Testometric M350-20KN tester at a speed of 10 mm/min at room temperature. Ultimate tensile strength, elongation at break, and Young's modulus were evaluated from stress–strain curves. Specimens were prepared according to those specified by the ASTM D 638.

RESULTS AND DISCUSSION

In the manufacturing of organic–inorganic nanocomposite materials like PP/clay, suitable compatibilizer is needed to make the incompatibles compatible. For this purpose, a compound coupling compatibilizer was first synthesized (Step 1, Scheme 1).

We first prepared the amide of PPgMA and APTS by condensation reaction of the amino group of APTS molecule with the anhydride group of PPgMA in xylene solution. The amide of PPgMA/APTS thus prepared possess triethoxy silyl group on the end of APTSs, which were linked to polymeric PP segment through maleic amide on PPgMA (Scheme 1). The

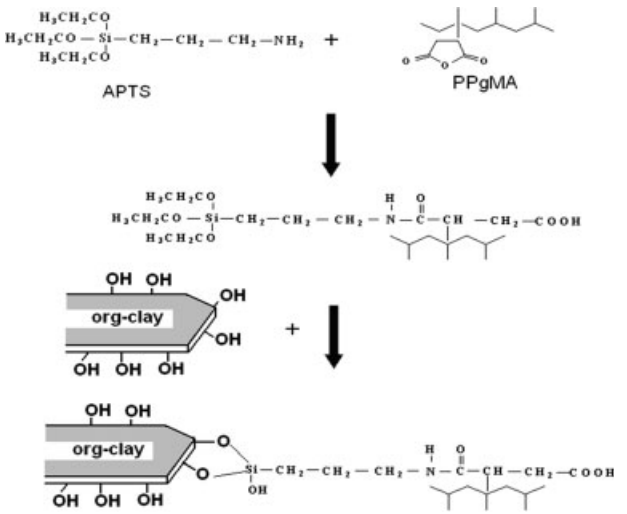

Scheme 1 The preparation of PPgMA/clay masterbatch.

condensation product is the PPgMA/APTS compound coupling compatabilizer. It was expected that the triethoxy silyl group of APTS is able to form covalent bonds with the hydroxyl groups on the edges of the layered silicate, while the polymeric PP segment of PPgMA can easily be entangled with the PP matrix.

The obtained amide (of PPgMA/APTS, the compound coupling compatabilizer) solution was further mixed with the suspension solution of org-clay (OTAC-modified clay) for the chemical reaction between the triethoxy silyl group on the PPgMA/APTS compatibilizer and the hydroxyl group of the layered silicate of the org-clay. The final condensation product was precipitated, washed, and dried, and a hybrid masterbatch of PPgMA/clay was obtained. The masterbatch has an organic (PPgMA)–inorganic (clay) with APTS as the covalent bond linker.

After Si—O—Si bond formation between APTS and the org-clay, the obtained PPgMA/clay masterbatch, as described earlier, still has the polymeric PP segment attached to maleic amide at the PPgMA end, which allow for subsequent compounding with pure PP to produce PP/clay hybrid nanocomposite. Different ratios between org-clay, PPgMA, and PP should render the nanocomposite different properties. The effects of these ratios on the physical properties of the final product were investigated by adjusting dosages.

In designing the PP/clay nanocomposite, the use of clay was for the purpose of modifying PP for desired properties, where PP is the major component and, relatively, clay will be minor. The role of APTS was to anchor the PPgMA/APTS compound coupling compatibilizer on the clay through Si—O—Si covalent bonding. Therefore, by adjusting the ratios

between org-clay, PPgMA, and PP, the amount of APTS was fixed at 1 wt %. Unreacted APTS will be washed off in the last step. The preparation scheme of PPgMA/clay hybrid masterbatch and PP/clay hybrid nanocomposites of various compositions are summarized in Table I.

FTIR characterization

FTIR is an important tool for observing the formation and/or disappearance of various chemical bonds. Compounds with characteristic functional groups often give special pattern FTIR spectrum. In this study, FTIR spectrum can deliver the information about bond formation in the preparation of the PPgMA/APTS compound coupling compatibilizer.

It has been reported that APTS can be attached to inorganic metal oxide, such as clay, by adsorption and Si—O—Si chemical bonding to form a mono molecular layer.[34,37,40] Details regarding this part will not be included in this report. Figure 1 compared the FTIR spectrum of the pure APTS, PPgMA, and the PPgMA/clay masterbatch. In the spectrum of APTS, the broad absorption with doublet peaks at high frequency around 3284 and 3353 cm^{-1} corresponds to the stretching mode of the primary amino group ($—NH_2$). For PPgMA, the C=O stretching mode of the anhydride group showed absorption peaks at 1782 and 1860 cm^{-1}. However, the absorption peaks aforementioned were not seen in the spectrum of the PPgMA/clay masterbatch, because of the condensation reaction between the amino group and the MA. Additionally, three absorption peaks around 1643 and 1589 cm^{-1} were found in the FTIR spectrum of the masterbatch corresponded to the C=O stretching vibration mode of amide (amide I band 1643 cm^{-1}) and N—H bending vibration mode of amide II band (1589 cm^{-1}). This comparison provided an evidence of the successful covalent bonding between PPgMA and APTS, and indicated that the anhydride ring of MA in PPgMA has been opened by the primary amino group in the APTS, a result similar to that of reports in the literature.[40,43,44]

Many researchers have shown that APTS can attach to inorganic metal oxide, such as clay, through adsorption and chemical bonding to form a mono molecular layer. In our case, APTS was to be anchored on the edge of layer silicate of the clay mineral according to Scheme 1. However, before reaction, IR absorption peaks corresponded to the Si—O—C bond in the triethoxy silyl groups reside in the neighborhood of 1086 cm^{-1}, which coincided with, and were buried in the strong broad peak (1094 cm^{-1}) representing the Si—O—Si bonds in the later formed PPgMA/clay masterbatch, which was the same as the data from the literature.[45]

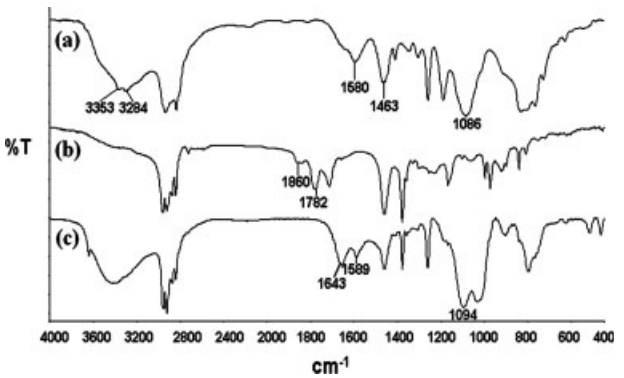

Figure 1 FTIR spectra of (a) pure APTS; (b) pure PPgMA; (c) PPgMA/clay masterbatch (PPgMA : APTS : clay = 10 : 1 : 3).

The strong broad peak of the Si—O—Si after the condensation of trialkylsilyl group of silane coupling agent with inorganic Si—OH was in the neighborhood of 1095 cm^{-1} in Wang's report,[34] 1090 cm^{-1} in Seckin et al.' report,[37] and 1029–1120 cm^{-1} in Barsbay's report.[40] Although, the Si—O—Si bond formation between the triethoxy silyl groups on APTS and silicate cannot be easily distinguished on the presented FTIR spectrum, as mentioned earlier, the Si—O—C and the Si—O—Si absorption peaks both occurred between 1100 and 1000 cm^{-1}; such bond formation has been witnessed by other researchers.[34,37,40] However, overlapped absorption peaks made it hard to obtain a clear distinction between the Si—O—C and the Si—O—Si bond absorptions in Figure 1.

Dispersity of clay

The XRD of pure clay, OTAC-modified clay, and pure PP are given in Figure 2(a). The interlayer distance in the clay could be calculated from the 2θ peak position, which corresponds to the (001) plane reflections of the clay. The pure sodium clay has a characteristic 2θ peak, corresponding to an average interlayer distance of ~ 12 Å. It is clear that the XRD curve shifts to a smaller angle of 2θ peak for the modified clay, indicating an increased interlayer distance in the modified clay. Based on the XRD curve of the OTAC-modified clay, the interlayer distance of the clay was ~ 20.4 Å. The alkylammonium ion exchange enables the conversion of the hydrophilic clay surface to hydrophobic in addition to increased interlayer distance. The OTAC-modified clay showed similar results and has been widely applied in the preparation of nanocomposites.

Figure 2(b) also compared the XRD scans of PP-clay nanocomposites in the presence of PPgMA/APTS compound coupling compatibilizer after being hot pressed into thin films. For all these PP/clay

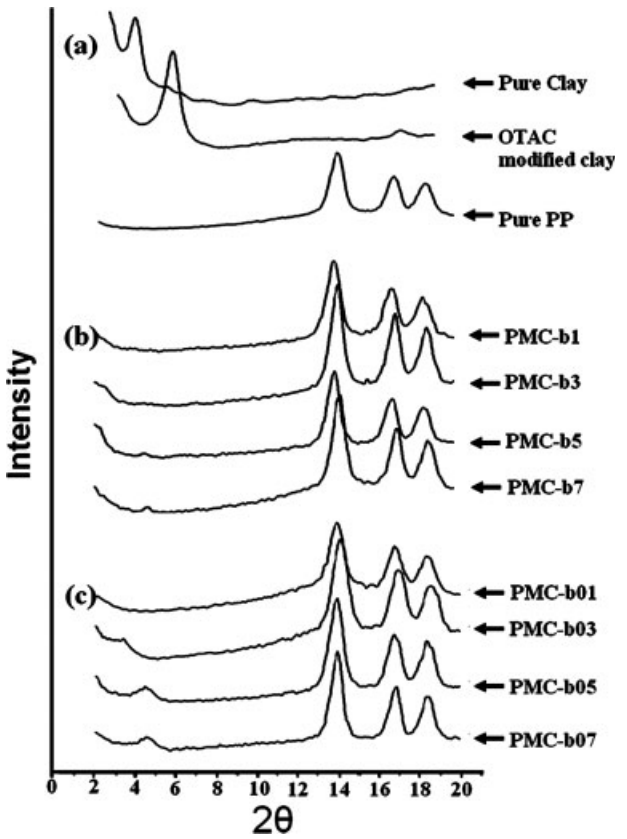

Figure 2 XRD patterns of (a) pure clay, OTAC-modified clay, pure PP, and PP/clay nanocomposites of (b) ''set-b'' and (c) ''set-b0.''

nanocomposites, XRD data showed three prominent 2θ peaks ranged in 10–20°, which corresponded to monoclinic α crystalline phase of PP.[46] These figures showed no significant variation in 2θ peaks between PP and PP/clay nanocomposites in this range. This indicated that the addition of clay did not affect the crystalline structure of the PP matrix in these nanocomposites.

On the other hand, in Figure 2(b), with org-clay content less than 5 wt % (in the presence of APTS), the 2θ peak between 2.5° and 10° disappeared (compared with the PMC-b7 curve). The disappearance of the characteristic 2θ peak suggests that the silicate layers in the PP/clay nanocomposites were no longer stacked together, for all ingredient ratios with org-clay content less than 5 wt %. However, for the PMC-b7 curve in Figure 2(b), there was a small peak at the same position as for the curve of OTAC-modified clay in Figure 2(a). This indicated a intercalated structure of the PMC-b7 nanocomposites. Figure 2(b) provided only XRD patterns for ''set-b'' (Table I, PMC-b1 to PMC-b7) for comparison, and this observation applied to ''set-a'' and ''set-c'' as well (data not shown).

The incompatibility between the inorganic clay and organic PP is commonly manifested by the tendency of the clay to aggregate in PP. One way to circumvent this problem is to modify the clay to manipulate its hydrophobicity. OTAC-modified clay is a good example; as shown in Figure 2(a), the 2θ peak shifted from 6°, for pure clay, to 4°, for OTAC-modified clay, indicating increased interlayer distance. Some successful applications of compounding clay with organic polymer using OTAC-modified clay could be found in the literature. However, such success has been limited to polar polymers.[10–15] For compounding with nonpolar PP, PPgMA has been suggested to be used as the compatibilizer. To some extent, PPgMA did contribute in making the two compatible. This works fine in some applications.[22,31] We speculated that a compound coupling compatibilizer, which is chemically anchored to the clay on one end, and possess a polymeric segment on the other end that is fully compatible with the polymer to be compounded with, would be another alternative to broaden the application of org-clay.

On basis of the above rationale, and what have been revealed by Figure 2(b), the APTS was chosen to be a bridging molecule in connecting PPgMA and org-clay by chemical bonding. Together with this, the thorough compatibility of PP segment in PPgMA with PP matrix would bring about exfoliation of the silicate layers of org-clay in PP matrix. However, according to Figure 2(b), in the presence of the PPgMA/APTS compound coupling compatibilizer, possible exfoliation was observed only when the org-clay content was lower than or equal to 5 wt %.

For comparison, the PP/clay nanocomposites with 10 wt % of PPgMA and different content of org-clay (1, 3, 5, 7 wt %), without APTS ("set-b0,'' from PMC-b01 to PMC-b07) were also subject to XRD study. The obtained results were shown in Figure 2(c). Except for PMC-b01 (which had the exfoliated structure), XRD curves for other nanocomposites of ''set-b0'' showed intercalated structure. In Figure 2(c), the 2θ peak (near 4°) shifted to higher degree, as the org-clay content was increased. This revealed that the interlayer distance decreased with increasing org-clay content. From the data of these two sets of PP/clay nanocomposites ("set-b'' and ''set-b0''), it is plausible to say that the addition of silane coupling agent in the design of the PPgMA/APTS compound coupling compatibilizer served to improve the dispersity of org-clay in PP/clay nanocomposites.

XRD curves provided information about the dispersion of clay. However, stronger evidences are needed for the judgment about a complete exfoliated structure. Cross-referencing XRD curves with TEM study would provide a basis for a more objective analysis. Figure 3 compared the TEM micrographs of PP/clay nanocomposites with 5 wt % of org-clay and silane coupling agent with different PPgMA contents. The dark lines depicted the cross section of

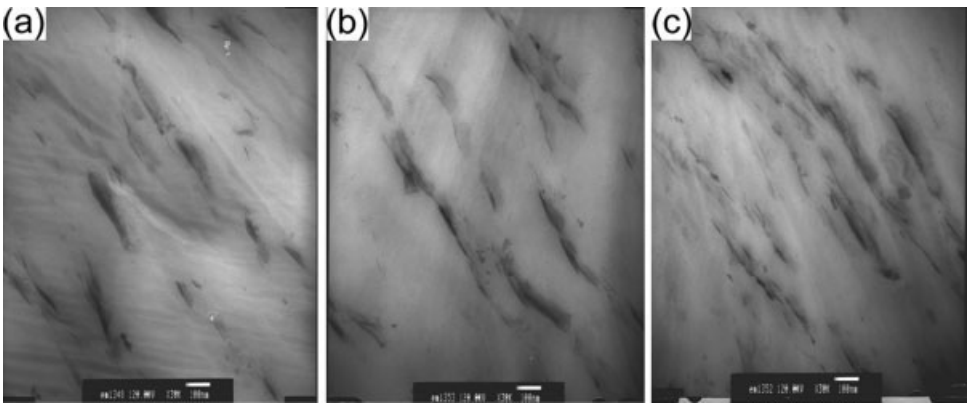

Figure 3 TEM images of PP/clay nanocomposites: (a) PMC-a5; (b) PMC-b5; (c) PMC-c5 (Table I).

silicate layers in the PP matrix. While XRD curves for PMC-b1, b3, b5 [Fig. 2(b)] showed a exfoliated structure, still some tactoids can be observed in the TEM micrographs (Fig. 3). It is quite likely that when the org-clay content was 5 wt %, the layered silicates, in the PP/clay nanocomposites, were in the form of ''intercalated-exfoliated'' structure.

Thermal properties

Figure 4 compared the DSC cooling scan thermograms of pure PP and PP/clay nanocomposites. The crystallization peak temperature (T_c) of pure PP was located at 110.0°C, which increased slightly as the org-clay content of the PP/clay nanocomposites was increased. The effect of increased T_c in the presence of org-clay could be explained by the possibility of the org/clay acting as an efficient nucleating agent for the crystallization of the PP matrix.

The role of org-clay in seeding the crystallization process in DSC study has been observed in a similar occasion in the literature[35,42] which led to the elevation of T_c (Table II, Fig. 4). During the course of temperature drop, the microscopic structure of the nanocomposite varied accordingly, from amorphous to crystalline structure.

On the other hand, when we increased the PPgMA content, the T_c of PP/clay nanocomposites were slightly decreased from ''set-a'' to ''set-c'' (Table II). The reason for such minor influence of PPgMA on T_c was not pursued in this research.

The TGA analysis provides important proofs in determining the thermal stabilities of the nanocomposites. The TGA curves as shown in Figure 5 depicted the variations of residual weight, of pure PP and PP/clay nanocomposites, versus temperature. The TGA curves in Figure 5 showed that there was a drastic shift of weight loss curve toward higher temperature. The decomposition temperatures (T_d) of pure PP and all of the nanocomposites were listed in Table II. These data exhibited marked increase of T_d for PP/clay nanocomposites, when compared with pure PP. The up shift of T_d of the PP/clay nanocomposites may be attributed to the formation of a highly charred carbonaceous-silicate cumulating on the nanocomposite surface. It is quite likely that, on one hand, the charred surface layer formed during decomposition shielded the thermal shock due to heat penetration to the underlying material, and on the other hand, such cumulated char layer tends to retard the escape of decomposed volatile products generated during thermal decomposition. In the nitrogen atmosphere, the amount of residue at high temperature (>550°C) was slightly higher for nanocomposites with higher org-clay content, which may be a result from the presence of clay *per se* in the clay-reinforced PP.

Dynamic mechanical properties

In the DMA study, the storage modulus (E') and the curves of tan δ versus temperature are very useful in determining the performances of materials under stress. Figure 6 compared the loss factor (tan δ) as a function of temperature for pure PP and PP/clay nanocomposites. The results showed that the differences between the PP/clay nanocomposites of various compositions were minor. This implies that the glass

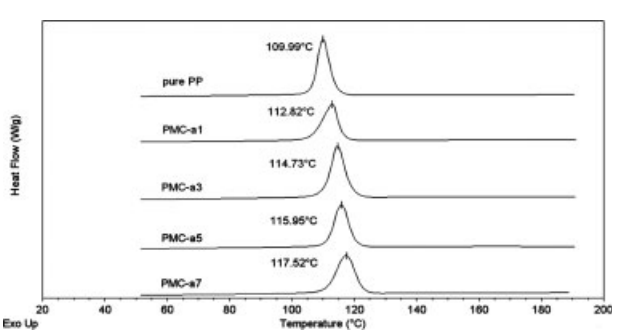

Figure 4 The DSC patterns of pure PP and PP/clay nanocomposites.

TABLE II
T_c, T_d, and Dynamic Mechanical Properties of Pure PP and PP/Clay Nanocomposites at Various Temperatures

Sample code	T_c[a] (°C)	T_d[b] (°C)	T_g (°C)	E'^c (MPa) 0°C	E'^c (MPa) 25°C	E'^c (MPa) 50°C
Pure PP	110.0	386.4	12.0	2214	1217	757
PMC-a1	112.8	460.3	11.1	1791	955	629
PMC-a3	114.7	478.8	10.6	2168	1214	786
PMC-a5	116.0	480.2	9.8	2816	1591	1005
PMC-a7	117.5	484.1	10.7	3578	2120	1422
PMC-b1	111.9	432.8	11.1	1984	996	526
PMC-b3	113.2	466.5	10.6	2092	1101	581
PMC-b5	114.3	470.9	9.4	2610	1391	816
PMC-b7	116.9	463.5	9.5	3381	1739	1051
PMC-c1	111.2	457.3	10.1	2353	1299	769
PMC-c3	112.4	471.9	10.8	2866	1639	948
PMC-c5	113.3	479.4	10.5	3168	1753	1008
PMC-c7	115.5	481.9	11.2	3673	2088	1277

[a] T_c was obtained by DSC analysis.
[b] T_d was the temperature of maximum slope in the TGA analysis.
[c] E' is the storage modulus.

transition temperatures (T_g, shown as the maximum of tan δ curves), as discussed by Wang and Sheng,[35] were not significantly affected by the incorporation of org-clay (Fig. 6). Similar observations regarding T_g have been reported by other researchers.[42]

Combining the DSC (Fig. 4) and DMA analyses, it was concluded similarly here, that it was the crystalline domain of the PP-clay nanocomposites, which was influenced by the presence of the org/clay (as evidenced by elevated T_c), while the amorphous regions were not (as shown by unchanged T_g).

The dynamic storage modulus (E') of pure PP and PP-clay nanocomposites versus the temperature were plotted in Figure 7. The storage modulus of the studied nanocomposites at 0, 25, and 50°C are summarized in Table II. These results showed that the E' of the PP/clay nanocomposites were higher than that of pure PP, indicating that the addition of PPgMA/clay masterbatch into PP matrix enhanced the stiffness and the reinforcing effect was remarkably good. In designing nanocomposite materials of this kind, it may be desirable to achieve different extent of reinforcement, depending on applications. According to Table II, the content of the incorporated layered silicates may be regarded as a design variable.

Mechanical properties

The intention of incorporating clay into the PP matrix was mainly for the purpose of improving its mechanical properties. The ultimate tensile strength, modulus, and elongation at break of PP/clay nanocomposites with different PPgMA and org-clay content, with and without silane coupling agent (APTS), were also measured. Table III listed the ultimate tensile strength of PP/clay nanocomposites at various org-clay and PPgMA content. From these data, it can be found that for the same PPgMA and APTS content, the ultimate tensile strength increased with increasing org-clay content. Meanwhile, the ultimate tensile strengths of PP/clay nanocomposite without

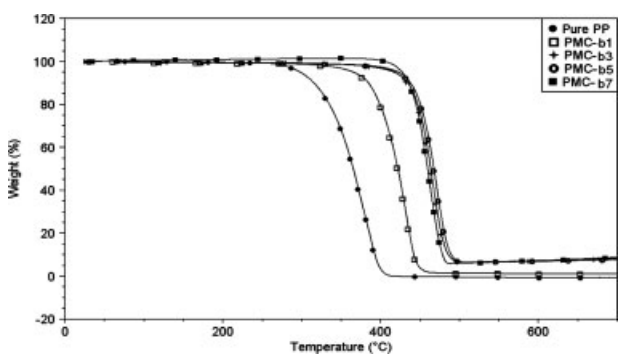

Figure 5 TGA curves of pure PP and PP/clay nanocomposites (''set-b'' in Table I).

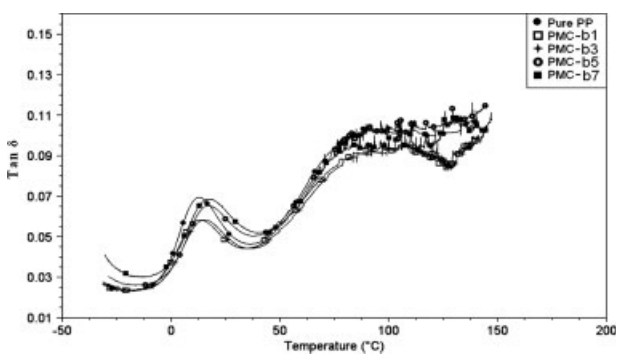

Figure 6 Tan δ of pure PP and PP/clay nanocomposites as a function of temperature (''set-b'' in Table I).

APTS (''set-b0,'' PMC-b01 to PMC-b07) were lower than those with APTS (''set-b,'' PMC-b1 to PMC-b7). This may be attributed to the presence of incorporated APTS which provided covalent linkage between the organic PP/PPgMA phase (the interpenetrated PP and PPgMA matrix) and the layered silicate phase.

Furthermore, with the same content of org-clay and silane coupling agent, the ultimate tensile strength also increased from ''set-a'' to ''set-c'' (Table III). Generally, in the absence of org-clay, the addition of PPgMA to PP was not supposed to increase the ultimate tensile strength (data were not shown). In this case, PPgMA, besides serving as a compatibilizer, together with APTS (after first compounding with APTS and org-clay), it also provides the important covalent linkage between organic and inorganic phases, and consequently increases the ultimate tensile strength (Table III). Comparing to pure PP, coupled use of APTS and PPgMA, up to 30% increase in ultimate tensile strength was obtained.

Elongation at break is also an important mechanical property for materials of this category. In general, the incorporation of org-clay in polymeric materials tends to reduce the elongation at break. As shown in Table III (sets a, b, c, and b0), the elongation at break of the nanocomposites of various org-clay contents followed this trend. The contribution of APTS could be observed by comparing ''set-b'' (with APTS, higher elongation) with ''set-b0'' (without APTS, lower elongation).

Table III also compared the Young's modulus of PP/clay nanocomposites with various org-clay and PPgMA content. Within the range of this study, for the same PPgMA content, the Young's modulus increased with increasing content of org-clay, and the same with increasing PPgMA while holding constant the org-clay content. The maximum value of Young's modulus in these prepared PP/clay nanocomposite was 57% higher than that of pure PP. APTS also contributed in enhancing the material's Young's modulus, and this can be seen in Table III by comparing the data for ''set-b'' (with APTS, higher modulus) with ''set-b0'' (without APTS, lower modulus).

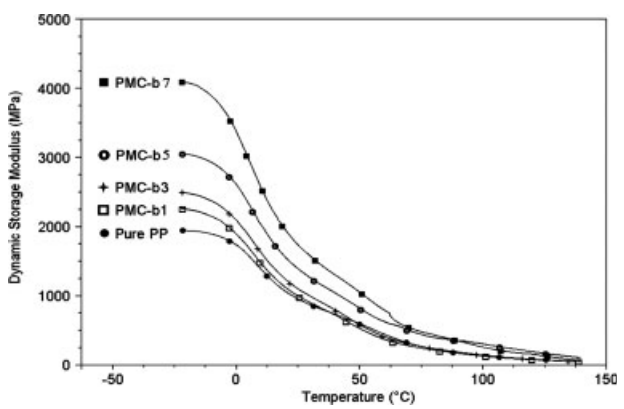

Figure 7 Storage modulus (E') curves of pure PP and PP/clay nanocomposites as a function of temperature (''set-b'' in Table I).

TABLE III
The Mechanical Properties of PP/Clay Nanocomposites

Sample code	Young's modulus (MPa)	Ultimate tensile strength (MPa)	Elongation at break (%)
Pure PP	1259 ± 35	32.7 ± 0.5	87 ± 2
PMC-a1	1382 ± 23	35.7 ± 0.4	84 ± 2
PMC-a3	1636 ± 39	37.2 ± 0.7	78 ± 3
PMC-a5	1805 ± 41	39.2 ± 0.8	72 ± 2
PMC-a7	1832 ± 52	39.8 ± 0.9	64 ± 2
PMC-b1	1426 ± 37	36.2 ± 0.5	90 ± 3
PMC-b3	1735 ± 42	39.3 ± 0.7	81 ± 2
PMC-b5	1913 ± 52	41.6 ± 0.9	78 ± 3
PMC-b7	1962 ± 49	41.9 ± 1.0	67 ± 2
PMC-c1	1393 ± 31	36.1 ± 0.7	89 ± 3
PMC-c3	1742 ± 36	40.7 ± 0.9	83 ± 2
PMC-c5	1975 ± 55	42.1 ± 0.8	81 ± 3
PMC-c7	1978 ± 58	42.4 ± 0.6	70 ± 2
PMC-b01	1384 ± 27	35.6 ± 0.5	81 ± 3
PMC-b03	1536 ± 32	37.2 ± 0.6	74 ± 2
PMC-b05	1623 ± 31	37.8 ± 0.9	65 ± 3
PMC-b07	1709 ± 36	38.2 ± 0.7	58 ± 3

It is worth mentioning here that in the effort to making the clay and PP compatible, the main strategy is through designing compatibilizer that is capable of chemically linking the two. Morphologically speaking, the adoption of the PPgMA/APTS compound coupling compatibilizer reduced the tendency of clay to aggregate in the PP matrix and allowed an intercalated-exfoliated structure (at 5 wt % org-clay) that provided a more uniformed reinforcement.

In this study, covalent bonds between the layered silicates of the clay and the triethoxy silyl groups on the synthesized PPgMA/APTS compound coupling compatabilizer, allowed the use of 5 wt % of clay with intercalated-exfoliated structure without serious aggregation. The ultimate tensile strength did not go down upon further increase of clay content to 7 wt %. This may serve as another partial proof that the synthesized compound coupling compatibilizer minimized the inherent interfacial incompatibility at the clay-PP boundary.

CONCLUSIONS

The PPgMA/APTS compound coupling compatibilizer, synthesized through simple condensation reaction, provided the opportunity of Si—O—Si covalent bond formation, in addition to stable C—Si bonds originally presented in the coupling agent, at the organic–inorganic interface. The C—Si covalent bond, together with the amide bond (formed between

PPgMA and APTS), provided a strong bridge that covalently linked the clay and the PP matrices. Such covalent bond linkage, to some extent, blurred the boundary between the organic and the inorganic worlds, as indicated by an intercalated-exfoliated structure at clay content of 5 wt %. Significant reinforcement of PP was achieved by compounding the PPgMA/clay masterbatch with PP at up to 5 wt % of org-clay.

References

1. Hu, X.; Zhao, X. Y. Polymer 2004, 45, 3819.
2. Kawasumi, M.; Hasegawa, N.; Kato, M.; Usuki, A.; Okada, A. Macromolecules 1997, 30, 6333.
3. Baron, P. C.; Wang, Z.; Pinnavaia, T. J Appl Clay Sci 1999, 15, 11.
4. Lee, H. S.; Fishman, D.; Kim, B.; Weiss, R. A. Polymer 2004, 45, 7807.
5. Novak, B. M. Adv Mater 1993, 6, 422.
6. Vaia, R. A.; Giannelis, E. P. Macromolecules 1997, 30, 8000.
7. Krishnamoorti, R.; Giannelis, E. P. Macromolecules 1997, 30, 4097.
8. Lyatskaya, Y.; Balazs, A. C. Macromolecules 1998, 31, 6676.
9. Palazs, A. C.; Singh, C.; Zhulina, E. Marcomolecules 1998, 31, 8370.
10. Usuki, A.; Kawasumi, M.; Kojima, Y.; Fukushima, Y.; Okada, A.; Kurauchi, T.; Kamigaito, O. J Mater Res 1993, 8, 1179.
11. Kojima, Y.; Usuki, A.; Kawasumi, M.; Kojima, Y.; Fukushima, Y.; Okada, A.; Kurauchi, T.; Kamigaito, O. J Mater Res 1993, 8, 1185.
12. Kojima, Y.; Usuki, A.; Kawasumi, M.; Kojima, Y.; Fukushima, Y.; Okada, A.; Kurauchi, T.; Kamigaito, O. J Polym Sci Part A: Polym Chem 1993, 31, 1755.
13. Lee, S. R.; Park, H. M.; Lim, H.; Kang, T.; Li, X.; Cho, W. J.; Ha, C. S. Polymer 2002, 43, 2495.
14. Davis, C. H.; Mathias, L. J.; Gilman, J. W; Schiraldi, D. A.; Shields, J. R.; Trulove, P.; Sutto, T. E.; Hugh, G. D. J Polym Sci Part B: Polym Phys 2002, 40, 2661.
15. Ke, Y. C.; Yang, Z. B.; Zhu, C. F. J Appl Polym Sci 2002, 85, 2677.
16. Mori, Y.; Saito, R. Polymer 2004, 45, 95.
17. Okamoto, M.; Morita, S.; Taguchi, H.; Kim, Y. H.; Kotato, T.; Tateyama, H. Polymer 2000, 41, 3887.
18. Liu, X.; Wu, Q. Polymer 2001, 42, 10013.
19. Zhang, Y. Q.; Lee, J. H.; Jang, H. J.; Nah, C. W. Composites Part B 2004, 35, 133.
20. Zilg, C.; Thomann, R.; Mülhaupt, R.; Finter, J. Adv Mater 1999, 11, 49.
21. Lan, T.; Pinnavaia, T. Chem Mater 1994, 6, 2216.
22. López-Quintanilla, M. L.; Sánchez-Valdés, S.; Ramos de valle, L. F.; Medellín-Rodríguez, F. J. J Appl Polym Sci 2006, 100, 4748.
23. Joen, H. G.; Jung, H. T.; Lee, S. D. Polym Bull 1998, 41, 107.
24. Zhu, L.; Xanthos, M. J Appl Polym Sci 2004, 93, 1891.
25. Manias, E.; Touny, A.; Wu, L.; Lu, B.; Strawhecker, K.; Guilman, J.; Chung, T. Polym Mater Sci Eng 2000, 82, 282.
26. Kato, M.; Usuki, A.; Okada, A. J Appl Polym Sci 1997, 66, 1781.
27. Hasegawa, N.; Kawasumi, M.; Kato, M.; Usuki, A.; Okada, A. J Appl Polym Sci 1998., 67, 87.
28. Wang, Y.; Chen, F. B.; Li, Y. C.; Wu, K. C. Composites Part B 2004, 35, 111.
29. Chiu, F. C.; Lai, S. M.; Chen, J. W.; Chu, P. H. J Polym Sci Part B: Polym Phys 2004, 42, 4139.
30. Usuki, A.; Kato, M.; Okada, A.; Kurauchi, T. J Appl Polym Sci 1997, 63, 137.
31. García-López, D.; Picazo, O.; Merino, J. C.; Pastor, J. M. Eur Polym J 2003, 39, 945.
32. Wu, J. Y.; Wu, T. M.; Chen, W. Y.; Tsai, S. J.; Kuo, W. F.; Chang, G. Y. J Polym Sci Part B: Polym Phys 2005, 43, 3242.
33. Rong, M. Z.; Ji, Q. L.; Zhang, M. Q.; Friedrich, K. Eur Polym J 2002, 38, 1573.
34. Wang, L.; Sheng, J. J Macromol Sci Part A: Pure Appl Chem 2003, 40, 1135.
35. Wang, L.; Sheng, J. Polymer 2005, 46, 6243.
36. Herrera, N. N.; Letoffe, J. M.; Putaux, J. L.; David, L.; Bourgeat-Lami, E. Langmuir 2004, 20, 1564.
37. Seckin, T.; Gültek, A.; Icduygu, M. G.; Önal, Y. J Appl Polym Sci 2002, 84, 164.
38. Lee, J. W.; Kim, M. H.; Choi, W. M.; Park, O. O. J Appl Polym Sci 2006, 99, 1752.
39. Zhao, C.; Feng, M.; Gong, F.; Qin, F.; Yang, M. J Appl Polym Sci 2002, 93, 676.
40. Barsbay, M.; Can, H. K.; Güner, A.; Rzaev, Z. M. O. Polym Adv Technol 2005, 16, 32.
41. Tanoue, S.; Hasook, A.; Itoh, T.; Yanou, M.; Iemoto, Y.; Unryu, T. J Appl Polym Sci 2006, 101, 1165.
42. Modesti, M.; Lorenzetti, A.; Bon, D.; Besco, S. Polym Degrad Stab 2006, 91, 672.
43. Park, H. B.; Kim, J. H.; Kim, J. K.; Lee, Y. M. Macromol Rapid Commun 2002, 23, 544.
44. Cornelius, C. J.; Marand, E. Polymer 2002, 43, 2385.
45. Silverstein, R. M.; Bassler, G. C.; Morrill, T. C. Spectrometric Identification of Organic Compounds; John Wiley & Sons, Inc.: Canada, 1981; p 175.
46. Saujanya, C.; Radhakrishnan, S. Polymer 2001, 42, 6723.